Simultaneous Needle Catheter Selection and Dwell Time Optimization for Preplanning of High-dose-rate Brachytherapy of Prostate Cancer

Chao Wang[1], Yesenia Gonzalez[1], Chenyang Shen[1], Brian Hrycushko[2], Xun Jia[1]

[1.] innovative Technology Of Radiotherapy Computation and Hardware (iTORCH) Laboratory, Department of Radiation Oncology, University of Texas Southwestern Medical Center, Dallas, TX 75390, USA
[2.] Department of Radiation Oncology, University of Texas Southwestern Medical Center, Dallas, TX 75287, USA

E-mails: xun.jia@utsouthwestern.edu

Purpose: Needle catheter positions critically affect the quality of treatment plans in prostate cancer high-dose-rate (HDR) brachytherapy. The current standard needle positioning approach is based on human intuition, which cannot guarantee a high-quality plan. This study proposed a method to simultaneously select needle catheter positions and determine dwell time for preplanning of HDR brachytherapy of prostate cancer.

Methods: We formulated the needle catheter selection problem and inverse dwell time optimization problem in a unified framework. In addition to the dose objectives of the planning target volume (PTV) and organs at risk (OARs), the objective function incorporated a group-sparsity term with a needle-specific adaptive weighting scheme to generate high-quality plans with the minimal number of needle catheters. The optimization problem was solved by a fast-iterative shrinkage-thresholding algorithm. For validation purposes, we tested the proposed algorithm on 10 patient cases previously treated at our institution and compared the resulting plans with plans generated using needle catheters selected manually.

Results: Compared to the plan with manually selected needle catheters, when normalizing both plans to the same PTV D_{95}, the plans generated by the proposed algorithm reduced median V_{125} from 70% to 62%, V_{150} from 34% to 26%, and V_{200} from 15% to 8%. The median homogeneity index and conformity index were increased from 0.64 to 0.74, and from 0.44 to 0.49, respectively. Most of clinically important dosimetric variables of OARs were reduced, except D_{1cc} and D_{2cc} of the rectum that were slight increased. On average, the number of selected needle catheters was reduced by two.

Conclusion: The proposed algorithm for prostate HDR brachytherapy preplanning was effective to perform needle catheter selection and dwell time optimization simultaneously.

1. INTRODUCTION

High-dose-rate (HDR) brachytherapy is an effective therapeutic approach for prostate cancer management, either as a monotherapy or as a boost in combination with external beam radiotherapy (Martinez *et al.*, 2001; Blasko *et al.*, 2002; Dinges *et al.*, 1998; Galalae *et al.*, 2002; Lachance *et al.*, 2002; Mate *et al.*, 1998; Thompson *et al.*, 2007; Yoshioka *et al.*, 2000). Different from external-beam radiotherapy that uses a high-energy radiation beam to deliver the dose from the outside of the patient's body, HDR brachytherapy delivers radiation directly to the tumor by having a radioactive source travel through catheter needles inserted into the prostate. This allows the achievement of a dose distribution highly conformal to the treatment targets, while effectively sparing surrounding normal organs.

In a typical procedure of prostate cancer HDR brachytherapy, a 2D template with a grid coordinate is used to define candidate needle catheter positions. A number of needle catheters in a subset of the candidate positions are inserted through the perineum to the treatment target under image guidance. After acquiring a 3D volumetric image for treatment planning, needle catheter trajectories are reconstructed, and dwell positions are determined along those trajectories. Finally, dwell times for each dwell position is optimized to generate a 3D dose distribution that meets clinical objectives. The quality of the resulting treatment plan depends on both the needle catheter positions and the optimized dwell times of the dwell positions defined within the needle catheters. Hence, a proper needle catheter configuration is the basis for a high-quality plan. On one hand, a sufficient number of needle catheters have to be inserted to achieve adequate dose coverage of the tumor while sparing adjacent normal organs. On the other hand, it is highly desired to use as a minimal number of needle catheters as possible to minimize trauma (Boyea *et al.*, 2007; Eapen *et al.*, 2004). The current clinical practice relies on physician's intuition to select needle catheter positions. While this has been acceptable as the standard practice, it is expected that the resulting needle catheter configuration would depend on physician's experience and may not guarantee an optimal treatment plan. Therefore, it is desirable to develop a method to guide the selection of needle catheter positions to ensure consistent achievement of high-quality plan for each patient.

A number of studies have been performed on the treatment planning problem of prostate cancer HDR brachytherapy, but most haven been focused on the optimization of dwell time for given dwell positions. Existing methods include simulated annealing (Deist and Gorissen, 2016; Lessard and Pouliot, 2001), particle swarm optimization (Moren *et al.*, 2018) and mixed integer programming as well as its convex relaxation (Moren *et al.*, 2019; Siauw *et al.*, 2011). Multi-criteria optimization (Breedveld *et al.*, 2019) and multi-resolution (Luong *et al.*, 2019) schemes have also been proposed. Relatively less research efforts have been devoted to the determination of optimal needle catheter positions. Sadowski et. al. employed a mixed-integer optimization approach with a genetic algorithm to solve this problem and found that clinically acceptable high-quality plans may be achievable with less catheters than typically used in the clinical practice (Sadowski *et al.*, 2017). Similarly, the Gene-pool Optimal Mixing Evolutionary Algorithm was used to

optimize catheter positions (van der Meer *et al.*, 2018). In (Siauw *et al.*, 2012), the authors reported a needle planning by integer program (NPIP) method to select needle catheters to meet the requirement of spatial coverage of the target.

The optimization problem for needle catheter selection belongs to the category of combinatorial optimization. The enormously large solution space prohibits the use of simple methods such as exhaustive search. Moreover, for this problem, the objective function defined for the independent variable of needle catheter configuration is indeed the optimal objective function value of the treatment planning optimization problem solved on top of the needle catheter configuration. This bi-level optimization structure further increases the difficulty of solving this problem in a mathematically rigorous form. In this paper, we propose an inverse planning method to perform needle catheter selection and dwell time optimization simultaneously for optimal plan quality with the minimal number of needle catheters selected. Our method will be based on the concept of group sparsity (Bach *et al.*, 2012; Bach, 2008; Huang and Zhang, 2010; Meier *et al.*, 2008; Simon *et al.*, 2013). Generally speaking, solving the group sparsity problem refers to the selection of a small number of groups of variables from candidate groups of variables to achieve a certain goal. In the context of HDR brachytherapy preplanning, all the independent variables of dwell time among all candidate needle catheters can be grouped based on the needle catheters. The group sparsity approach generates a solution that is sparse at the group level, i.e. the needle level, hence achieving the objectives of using a small number of needle catheters to produce a high-quality treatment plan. This group sparsity method has been successfully implemented in various applications (Parvaresh *et al.*, 2008; Wu and Lin, 2006), including beam orientation optimization in radiation therapy (Jia *et al.*, 2011; Gu *et al.*, 2018; Gu *et al.*, 2019; O'Connor *et al.*, 2017).

2. METHODS AND MATERIALS

2.1 Optimization problem

We considered the treatment planning problem with a 3D volumetric ultrasound image. Planning Target Volume (PTV) and Organs at Risk (OARs) including bladder, rectum, and urethra were delineated by the physician. The PTV was defined as prostate minus urethra. One additional structure generated for this study was a ring-shape protected zone around the PTV. The distance between the inner side of the ring and the PTV surface was 5 mm, and the thickness of the ring was 5 mm. Any overlapping region with OARs were removed from the protected zone. The purpose of generating this structure was to help enforcing dose fall-off outside the PTV, when solving the plan optimization problem.

We considered the setup using a 2D needle template (Eckert & Ziegler Group, Berlin, Germany) with a grid size of 13 × 13 needle catheters spaced 5 mm apart in the x-y direction. We first aligned the template with the patient anatomy. The template was assumed to be placed parallel to the axial image direction. Laterally, the grid center was aligned with the rectum center, and the posterior needle level was at the anterior side of the rectal wall (Fig. 1) to approximate the clinical setup with transrectal ultrasound (TRUS).

We assumed that needle catheters were inserted perpendicular to the template. Among the 169 possible needle catheter positions, we considered candidate needle catheter positions that resulted in needle catheters intersecting with a volume including the PTV with a 3mm outward expansion to provide sufficient dose coverage to PTV boundary. Hence, the number of candidate needle catheters was patient dependent. In our study, this number ranged between 50 and 74. Fig. 1 illustrates the geometry showing the candidate needle catheter positions relative to the PTV and OAR regions. For all the candidate needle catheters, dwell positions are placed along the needle catheters within the expanded prostate volume. This assumes each candidate needle catheter can be inserted sufficiently deep such that needle tips pass beyond the superior end of the prostate. The dwell positions were spaced 5mm apart following the setup of our Varian VariSource HDR brachytherapy afterloader (Varian Medical System, Palo Alto, CA, USA).

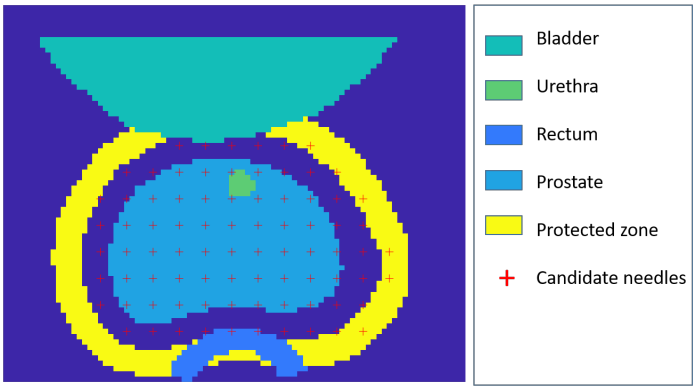

Figure 1: Illustration of candidate needle catheter positions relative to PTV and OARs.

The inverse planning task was formulated as solving an optimization problem that simultaneously selects the needle catheters and optimizes dwell time for corresponding sources in selected needle catheters. The objective function contains two parts. The first part describes dosimetric objectives. We consider a quadratic objective function that enforces PTV coverage close to the prescription dose, while minimizing doses to OARs:

$$\frac{1}{2}\left\|D_0\mathbf{t} - d_p\mathbf{1}\right\|_2^2 + \sum_{i=1}^{M}\frac{\lambda_i}{2}\left\|D_i\mathbf{t}\right\|_2^2, \quad (1)$$

where $\mathbf{t} = [\mathbf{t}_1; \mathbf{t}_2; \mathbf{t}_3; \ldots; \mathbf{t}_N] \geq \mathbf{0}$ denotes dwell time of a set of N candidate needle catheters, while the vector $\mathbf{t}_j$ specifies the dwell time for a number of n_j sources in the j-th candidate needle catheter. The matrix D_i is the dose-deposition matrix for the PTV ($i = 0$) or the OARs ($i = 1, 2, \ldots, M$), which specifies the contributions to dose at each voxel of the structure i from each dwell position at its unit time. Dose was calculated using the clinical standard AAPM TG-43 formalism (Rivard *et al.*, 2004). $\mathbf{1}$ and $\mathbf{0}$ are vectors with all elements being 1 or 0, respectively. The first term $\frac{1}{2}\left\|D_0\mathbf{t} - d_p\mathbf{1}\right\|_2^2$ enforces the PTV dose to be close to the prescription dose d_p, while the second term $\sum_{i=1}^{M}\frac{\lambda_i}{2}\|D_i\mathbf{t}\|_2^2$ penalizes

for dose to OARs. $\{\lambda_i\}$ is a set of parameters balancing the contributions among different terms in the objective function.

In addition to the terms specifying dosimetric objectives for the PTV and OARs, we incorporate a group-sparsity term to penalize for the number of selected needle catheters. More specifically, we chose an objective function of a weighted $L_{2,1}$ norm of $\mathbf{t}$:

$$\sum_{j=1}^{N} \mu_j \left\|\mathbf{t}_j\right\|_2, \tag{2}$$

where μ_j is the weighting factor of the j-th needle catheter. This $L_{2,1}$ norm first calculates the L_2 norm of the dwell time within each needle catheter group and then sums over all needle catheters in the L_1 norm. Minimizing the $L_{2,1}$ norm enforces the sparsity of the solution at the group (needle catheter) level, but not at the level of individual elements (dwell time) within each group. Hence, including this term in the objective function will promote a solution with only a small fraction of the candidate needle catheters containing non-zero dwell time to meet the dosimetric objectives, therefore accomplishing the goal of needle catheter selection. Combining these two objectives in Eq. (1) and (2), the proposed optimization problem was formulated as:

$$\min_{\boldsymbol{t}\geq\mathbf{0}} \frac{1}{2}\left\|D_0\mathbf{t} - d_p\mathbf{1}\right\|_2^2 + \sum_{i=1}^{M}\frac{\lambda_i}{2}\left\|D_i\mathbf{t}\right\|_2^2 + \sum_{j=1}^{N}\mu_j\left\|\mathbf{t}_j\right\|_2. \tag{3}$$

2.2. Optimization algorithm

The proposed optimization problem in Eq. (3) is convex and can be solved efficiently by a number of fast algorithms. In this study, we used the fast-iterative shrinkage-thresholding algorithm (FISTA) (Beck and Teboulle, 2009). FISTA considers a general minimization problem in the form of

$$\min_x f(x) + g(x),$$

where f is differentiable and convex, while g has an explicit form of its proximal operator. The iterative scheme in the k-th iteration is

$$\begin{cases} x^{(k)} = \mathrm{prox}_{\beta g}\left(y^{(k)} - \beta\nabla f\left(y^{(k)}\right)\right) \\ s^{(k+1)} = \dfrac{1+\sqrt{1+4(s^{(k)})^2}}{2} \\ y^{(k+1)} = x^k + \left(\dfrac{s^{(k)}-1}{s^{(k+1)}}\right)\left(x^{(k)} - x^{(k-1)}\right) \end{cases},$$

where the proximal operator is defined as $\mathrm{prox}_{\beta g}(x) = \min_u\left\{\beta g(u) + \frac{1}{2}\|u-x\|_2^2\right\}$ and β is a parameter. Specific to the problem of Eq. (3), we have $f(\mathbf{t}) = \frac{1}{2}\left\|D_0\mathbf{t} - d_p\mathbf{1}\right\|_2^2 + \sum_{i=1}^{M}\frac{\lambda_i}{2}\left\|D_i\mathbf{t}\right\|_2^2$, and $g(\mathbf{t}) = \sum_{j=1}^{N} g_j\left(\mathbf{t}_j\right)$, where

$$g_j\left(\mathbf{t}_j\right) = \begin{cases} \mu_j\left\|\mathbf{t}_j\right\|_2 & \mathbf{t}_j \geq 0, \\ \infty & \text{otherwise.} \end{cases}$$

Based on the chain rule, the gradient of f can be expressed as

$$\nabla f(\mathbf{t}) = D_0^T\left(D_0\mathbf{t} - d_p\mathbf{1}\right) + \sum_{i=1}^{M}\lambda_i D_i^T D_i\mathbf{t}.$$

Since g_j is separable, the proximal operator of g is given by

$$\text{prox}_g(\mathbf{t}) = \begin{pmatrix} \text{prox}_{g_1}(\mathbf{t}_1) \\ \text{prox}_{g_2}(\mathbf{t}_2) \\ \vdots \\ \text{prox}_{g_N}(\mathbf{t}_N) \end{pmatrix}.$$

According to (O'Connor *et al.*, 2017),

$$\text{prox}_{g_j}\left(\mathbf{t}_j\right) = \text{prox}_{\mu_j\|\cdot\|_2}\left(\max\left(\mathbf{t}_j, \mathbf{0}\right)\right).$$

Hence, the proximal operator of the L_2 norm is $\text{prox}_{\mu_j\|\cdot\|_2}(\mathbf{y}) = \mathbf{y} - P_j\mathbf{y}$, where $P_j\mathbf{y}$ denotes the projection of $\mathbf{y}$ onto the L_2 norm ball with a radius of μ_j, i.e.,

$$P_j\mathbf{y} = \begin{cases} \mu_j\mathbf{y}/\|\mathbf{y}\|_2 & \text{if } \|\mathbf{y}\|_2 > \mu_j, \\ \mathbf{y} & \text{otherwise.} \end{cases}$$

The iterative process of the algorithm is summarized in Algorithm 1.

Algorithm 1. FISTA algorithm solving the problem in (3).

Input: $D_i, \lambda_i, \mu_j, i = 0, 1, \ldots, M, j = 1, 2, \ldots, N$ and prescription dose d_p
Initialize: $\mathbf{y}^{(1)} = \mathbf{t}^{(0)}, s^{(1)}$, and step size β, tolerance σ
Output: $\mathbf{t}^*$
for $k = 1, 2, \ldots,$ **do**
$\mathbf{v}^{(k)} = \mathbf{y}^{(k)} - \beta\nabla f\left(\mathbf{y}^{(k)}\right)$, $\mathbf{v}^{(k)}$ is partitioned as $\mathbf{v}^{(k)} = \left[\mathbf{v}_1^{(k)}, \mathbf{v}_2^{(k)}, \ldots, \mathbf{v}_N^{(k)}\right]$
$\mathbf{t}_j^{(k)} = \text{prox}_{\beta\mu_j\|\cdot\|_2}\left(\max\left(\mathbf{v}_j^{(k)}, \mathbf{0}\right)\right),\ j = 1, 2, \ldots, N$
$\mathbf{t}^{(k)} = \left[\mathbf{t}_1^{(k)}, \mathbf{t}_2^{(k)}, \ldots, \mathbf{t}_N^{(k)}\right]$
$s^{(k+1)} = \frac{1+\sqrt{1+4\left(s^{(k)}\right)^2}}{2}$
$\mathbf{y}^{(k+1)} = \mathbf{t}^{(k)} + \left(\frac{s^{(k)}-1}{s^{(k+1)}}\right)\left(\mathbf{t}^{(k)} - \mathbf{t}^{(k-1)}\right)$
break if $\left\|\mathbf{t}^{(k)} - \mathbf{t}^{(k-1)}\right\|_2 / \left\|\mathbf{t}^{(k)}\right\|_2 < \sigma$, set $\mathbf{t}^* = \mathbf{t}^{(k)}$.
end for

2.3 Adaptive needle weight adjustment

Looking at the Algorithm 1, in each iteration, the operation $\max\left(\mathbf{v}_j, \mathbf{0}\right)$ eliminates negative elements in the solution vector. The proximal operator further reduces the magnitude of the solution for each needle catheter group. These operations gradually generate a sparsity solution in this iterative process. Importantly, the proximal operation projects the solution to a sphere having a radius of μ_j for the dwell time vector of needle catheter j. Proper selection of parameter μ_j could in principle accelerate the process of generating sparsity and hence the optimization process. Unfortunately, it is not possible to rigorously set the parameter values without knowing prior information. In (Ahmad and Schniter, 2015; Li *et al.*, 2017), the authors proposed an iterative weight adjustment scheme. The basic idea was to set a small weighting factor for the group that is likely to exist in the

final solution. The small weight for the group would then reduce the penalty of sparsity of this term in the objective function, hence preserving this group in the solution.

In light of this idea, we proposed a heuristic method for needle weight adjustment. Again, the basic idea is to estimate the importance of each needle catheter based on the intermediate solution $\mathbf{t}_j^{(k)}$ during the iterative process and assign smaller weights to those needle catheters that are likely more important. Specifically, we set the same weight for all the candidate needle catheters at the beginning of the iterative process and solve the problem with the fixed weight using FISTA for a number of iteration steps to obtain an estimate of the final solution. In practice, we found the first 100 iterative steps could lead to a reliable estimation. The weight is then updated adaptively at each step of the remaining iterations. Similar to (Ahmad and Schniter, 2015; Li *et al.*, 2017), the update was based on the $\left\|\mathbf{t}_j^{(k)}\right\|_2$, the L_2 norm of the intermediate solution in the k-the iteration, in the form of

$$\mu_j^{(k)} = c/\left(\left\|\mathbf{t}_j^{(k)}\right\|_2^2 + \epsilon\right), \tag{4}$$

where c is an overall constant that governs the trade-off between the sparsity objective and the dosimetric objective in the objective function. A relatively large $\left\|\mathbf{t}_j^{(k)}\right\|_2^2$ indicates that the needle catheter j is likely more important, and hence its weight is set to be small. $\epsilon > 0$ is a parameter with a small value to avoid divergence when computing $\mu_j^{(k)}$ for those needle catheters with zero dwell time. The adapted scheme is summarized in Algorithm 2.

Algorithm 2. FISTA algorithm solving the problem in (3) with the adaptive needle weights.

Input: $D_i, \lambda_i, i = 0, 1, \dots, M, c$ and prescription dose d_p
Initialize: $\mathbf{y}^{(1)} = \mathbf{t}^{(0)}, s^{(1)}$, and step size β, tolerance σ, ϵ
Output: $\boldsymbol{t}^*$
for $k = 1, 2, \dots, 100$ **do**
$\mathbf{v}^{(k)} = \mathbf{y}^{(k)} - \beta\nabla f\left(\mathbf{y}^{(k)}\right)$, $\mathbf{v}^{(k)}$ is partitioned as $\mathbf{v}^{(k)} = \left[\mathbf{v}_1^{(k)}, \mathbf{v}_2^{(k)}, \dots, \mathbf{v}_N^{(k)}\right]$
$\mathbf{t}_j^{(k)} = \text{prox}_{\beta c\|\cdot\|_2}\left(\max\left(\mathbf{v}_j^{(k)}, \mathbf{0}\right)\right),\ j = 1, 2, \dots, N$
$\mathbf{t}^{(k)} = \left[\mathbf{t}_1^{(k)}, \mathbf{t}_2^{(k)}, \dots, \mathbf{t}_N^{(k)}\right]$
$s^{(k+1)} = \frac{1+\sqrt{1+4\left(s^{(k)}\right)^2}}{2}$
$\mathbf{y}^{(k+1)} = \mathbf{t}^{(k)} + \left(\frac{s^{(k)}-1}{s^{(k+1)}}\right)\left(\mathbf{t}^{(k)} - \mathbf{t}^{(k-1)}\right)$
end for
for $k = 101, 102, \dots$ **do**
$\mathbf{v}^{(k)} = \mathbf{y}^{(k)} - \beta\nabla f\left(\mathbf{y}^{(k)}\right)$, $\mathbf{v}^{(k)}$ is partitioned as $\mathbf{v}^{(k)} = \left[\mathbf{v}_1^{(k)}, \mathbf{v}_2^{(k)}, \dots, \mathbf{v}_N^{(k)}\right]$
$\mathbf{t}_j^{(k)} = \text{prox}_{\beta\mu_j^{(k)}\|\cdot\|_2}\left(\max\left(\mathbf{v}_j^{(k)}, \mathbf{0}\right)\right),\ j = 1, 2, \dots, N$
$\mathbf{t}^{(k)} = \left[\mathbf{t}_1^{(k)}, \mathbf{t}_2^{(k)}, \dots, \mathbf{t}_N^{(k)}\right]$
$s^{(k+1)} = \frac{1+\sqrt{1+4\left(s^{(k)}\right)^2}}{2}$
$\mathbf{y}^{(k+1)} = \mathbf{t}^{(k)} + \left(\frac{s^{(k)}-1}{s^{(k+1)}}\right)\left(\mathbf{t}^{(k)} - \mathbf{t}^{(k-1)}\right)$

$\mu_j^{(k)} = c/\left(\left\|\mathbf{t}_j^{(k)}\right\|_2^2 + \epsilon\right)$;

break if $\left\|\mathbf{t}^{(k)} - \mathbf{t}^{(k-1)}\right\|_2 / \left\|\mathbf{t}^{(k)}\right\|_2 < \sigma$, set $\mathbf{t}^* = \mathbf{t}^{(k)}$.

end for

2.4 Evaluation studies

We tested the proposed method on a set of ten patient cases that were randomly selected from those patients treated at our institution. The prescription dose was either 14 Gy per fraction or 15 Gy per fraction depending on the specific treatment regimen for the patient. We extracted the PTV and OAR contours for each case from our clinical treatment planning system. We then discretized the volumetric space into voxels with 1 mm^3 in size. The number of voxels of PTV and OARs and their volumes are summarized in Table 1. For each case, we solved the preplanning problem using the proposed algorithm. In the optimization process, overlap between urethra and bladder is considered as urethra to give it higher priority. However, dose in overlapping voxels is considered in both organs when evaluating the resulting plans.

Table 1: Numbers of voxels and volumes of PTV and OARs in patient cases.

	Number of voxels		Volume	
	Mean	Range	Mean (cc)	Range (cc)
PTV	32023	22275 - 43701	32.02	22.28 - 43.70
Urethra	746	329 - 1234	0.75	0.33 - 1.23
Rectum	14971	7231 - 31882	1.50	7.23 - 31.88
Bladder	38389	12618 - 61745	38.51	12.70 - 61.90

To demonstrate the effectiveness of the proposed algorithm, we compared the optimized plans with the clinically used plans generated using needle catheter positions manually selected by the physicians during the actual HDR brachytherapy procedure. As such, we first identified the selected needle catheter positions for each patient case. Assuming the ideal needle catheter insertion situation with needles being perpendicular to the template, we positioned dwell positions inside the PTV and a 3mm expansion as previously described. After that, we solved an optimization problem with the group-sparsity term removed from Eq. (3), namely

$$\min_{\boldsymbol{t}\geq\mathbf{0}} \frac{1}{2}\left\|\widehat{D}_0\mathbf{t} - d_p\mathbf{1}\right\|_2^2 + \sum_{i=1}^{M}\frac{\lambda_i}{2}\left\|\widehat{D}_i\,\mathbf{t}\right\|_2^2. \tag{5}$$

Here $\widehat{D}_0$ and $\widehat{D}_i$ are dose deposition matrices for the known needle catheters. Because the known needle catheter positions belonged to the candidate needle catheter positions, $\widehat{D}_0$ and $\widehat{D}_i$ were submatrices of D_0 and D_j. We solved the problem of Eq. (5) by FISTA as well. Here,

$$f(\mathbf{t}) = \frac{1}{2}\left\|\widehat{D}_0\mathbf{t} - d_p\mathbf{1}\right\|_2^2 + \sum_{i=1}^{M}\frac{\lambda_i}{2}\left\|\widehat{D}_i\,\mathbf{t}\right\|_2^2,$$

and

$$g(\mathbf{t}) = \begin{cases} 0 & \mathbf{t} \geq \mathbf{0}, \\ \infty & otherwise. \end{cases}$$

$\text{prox}_g(y)$ is a nonnegative projection, i.e., $\text{prox}_g(\mathbf{y}) = \max(\mathbf{y}, 0)$. Therefore, the iterative scheme is

$$\begin{cases} \mathbf{t}^{(k)} = \max\left(\mathbf{y} - \beta\widehat{D}_0^T\left(\widehat{D}_0\mathbf{y}^{(k)} - d_p\mathbf{1}\right) - \sum_{i=1}^{M}\beta\lambda_i\widehat{D}_i^T\widehat{D}_i\mathbf{y}^{(k)}, \quad 0\right) \\ s^{(k+1)} = \dfrac{1+\sqrt{1+4(s^{(k)})^2}}{2} \\ \mathbf{y}^{(k+1)} = \mathbf{t}^{(k)} + \left(\frac{s^{(k)}-1}{s^{(k+1)}}\right)\left(\mathbf{t}^{(k)} - \mathbf{t}^{(k-1)}\right). \end{cases}$$

All the numerical experiments were conducted on a desktop computer equipped with a CPU (Intel i7- 6700, 3.4GHz) and 32 GB memory. We implemented all the computations using MATLAB 9.2 (R2017a) (MathWorks, Natick, MA, USA).

To evaluate the resulting plan quality and fairly compare qualities of plans, we normalized the plan generated by the proposed algorithm (Algorithm 2), such that its PTV D_{95} equaled to that of the plan generated using pre-determined needle catheters. In addition to examining typical dosimetric quantities of interest of the PTV and OARs, PTV homogeneity and conformality were also evaluated. Homogeneity Index (HI) was used to measure the dose homogeneity inside PTV(Major *et al.*, 2017), which was defined as

$$\text{HI} = 1 - V_{150}/V_{100}.$$

Conformity Index (CI) quantified the geometric congruence between the volume irradiated and the PTV volume (Cirino *et al.*, 2012). We considered the definition

$$\text{CI} = \frac{V_{\text{PTV}\geq d_p}}{V_{\text{PTV}}} \cdot \frac{V_{\text{PTV}\geq d_p}}{V_{total\geq d_p}}.$$

Here V_{PTV} is the PTV volume and $V_{\text{PTV}\geq d_p}$ is the volume of PTV receiving at least the prescribed dose d_p. $V_{total\geq d_p}$ represents the total volume receiving at least d_p.

3. RESULTS

3.1 Iteration process

We first present the iteration process for a representative patient case, in which the proposed algorithm gradually selects needle catheters. Fig. 2 shows the value of the objective function and the number of active needle catheters (needle catheters with non-zero dwell time) for each iteration. In the first 100 iterations, the weights for all the candidate needle catheters are the same and the objective function value dramatically decreases. However, the number of active needle catheters was only reduced slightly. After the first 100 iteration steps, the adaptive weight adjustment was turned on to accelerate the needle catheter selection process. In Fig.1(b), we can see that the number of active needle catheters was reduced rapidly by 32 from the 100-th iteration step to the 118-th iteration steps. The heuristic weight-adjustment scheme led to an increase of the objective function value after the first 100 iteration steps. The objective function value gradually saturates to

the final level. During this process, the number of active needle catheters is continuously reduced, finally saturating at 13 needle catheters.

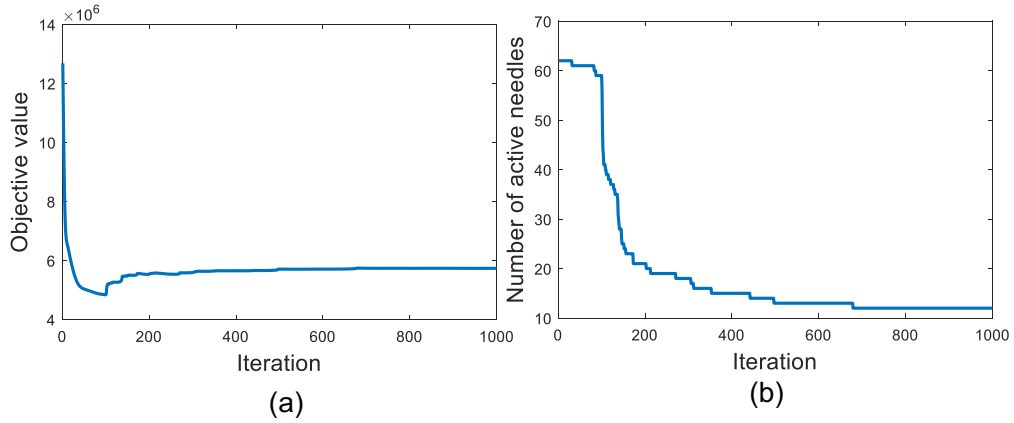

Figure 2: (a) Objective functions and (b) the number of active needle catheters during the iterative process.

We further demonstrate the effect of adaptive weight adjustment by comparing the needle catheter selection process using algorithms with (Algorithm 2) and without (Algorithm 1) the adaptive weight adjustment scheme. The number of active needle catheters during the iterative processes in these two cases are shown in Fig. 3. The one without adaptive weight cannot effectively reduce the number of the active needle catheters after the first 100 iterations, yielding a solution that can minimize the dosimetric objective function but with a relatively large number of needle catheters selected (59). In contrast, the adaptive weight adjustment scheme was able to dramatically reduce the needle catheter number to 13.

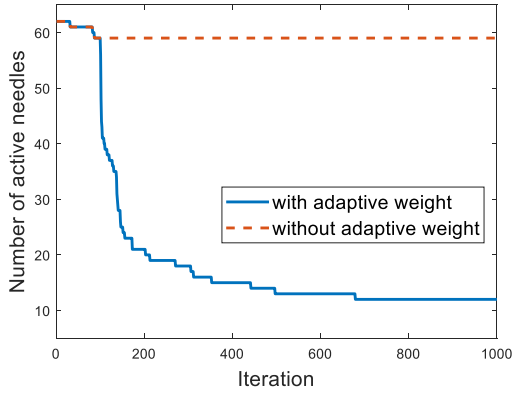

Figure 3: The number of active needle catheters in the iterative processes with/without the adaptive weight adjustment scheme.

3.2 Quantitative evaluations of plan quality

Using another patient case as an example, in Fig. 4, we compare the selected needle catheters, isodose lines, and dose volume histograms (DVHs) of the plan generated by the proposed algorithm with those in the plan optimized with needle catheters manually selected. The advantage of the proposed method can be clearly observed. The plan with

manually selected needle catheter positions contained 16 needle catheters. However, the needle catheters missed the superior-right and superior-left regions of the PTV. As a consequence, to a generate sufficient PTV coverage, the optimization algorithm had to increase some of the dwell time, yielding a relatively large connected hot region with dose greater than 150% of the prescription dose. In contrast, the proposed algorithm selected 13 needle catheters spanning the PTV region relatively uniformly and avoiding the urethra. The dose distribution was found to be more homogeneous compared to the other plan, as indicated by a few disconnected hot regions with relatively smaller sizes.

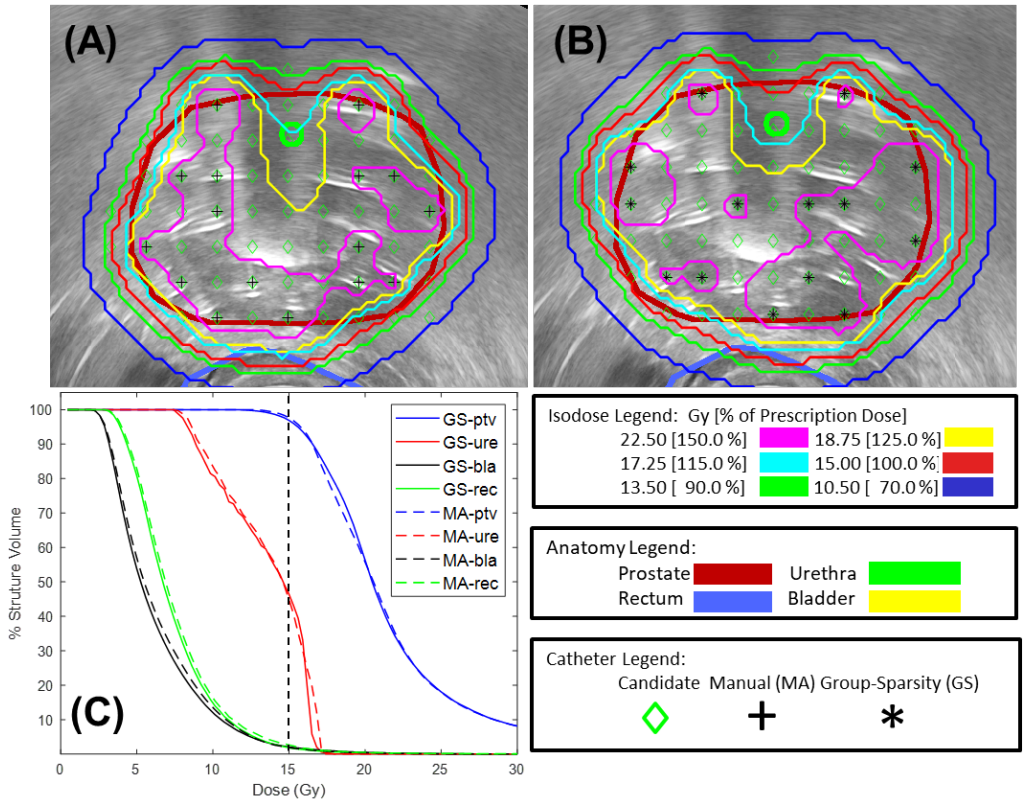

Figure 4: Selected needle catheters and isodose lines in the plan optimized with manually selected needle catheters (A) and the plan generated by our algorithm (B). The needle catheter positions and isodose lines are plotted over the ultrasound image and organ contours. (C) DVHs of these two plans. Prescription dose for this case was 15 Gy, as indicated by the vertical dash line.

In terms of DVH comparisons, the DVH of the PTV for the plan generated by the proposed algorithm was slightly sharper than that of the plan using pre-defined needle catheter positions, indicating better dose homogeneity. The dose to OARs were also reduced slightly. In particular, the hot spot of the urethra was reduced, which can also be observed by comparing the isodose lines. The 115% isodose line in the plan generated by the proposed algorithm curved around the urethra to effectively spare it.

Tables 2 and 3 summarize the median values of the dosimetric quantities of interest for all ten patient cases. We further present these metrics in Fig. 5 and 6 to better visualize the distributions among these patient cases. For PTV coverage, the V_{100} of the plan generated by the proposed algorithm was higher than that of the plan with manually selected needle

catheter positions. The other three quantities, V_{125}, V_{150}, and V_{200}, of the plan with needle catheters selected by our algorithm were all lower than the corresponding quantities in the clinically used plan. These numbers indicated the effectiveness of the proposed algorithm in terms of selecting needle catheters to generate plans with high PTV homogeneity. This was confirmed by the improvement of median HI from 0.64 to 0.74. The median CI was also improved, which was ascribed by the more appropriate needle catheter positions selected by the algorithm to allow a rapid dose fall-off outside the PTV. Note that these improvements were achieved with a median reduction of needle catheter number by 2. As for the quantities of interest for OARs, the proposed algorithm was able to reduce median values for all except the D_{1cc} and D_{2cc} of the rectum, which were increased slightly.

Table 2: PTV coverage metrics, homogeneity index (HI), Conformity Index (CI) and the number of needle catheters for the plan optimized with manually selected needle catheters (MA) and plan optimized using the proposed group sparsity algorithm (GS).

Method	Prostate (PTV)				HI	CI	No. of Needle catheters
	V_{100}	V_{125}	V_{150}	V_{200}			
MA	94%	70%	34%	15%	0.64	0.44	14
GS	96%	62%	26%	8%	0.74	0.49	12

Table 3: OARs dosimetric quantities of interest for the plan optimized with manually selected needle catheters (MA) and plan optimized using the proposed group sparsity algorithm (GS).

Method	Urethra		Bladder		Rectum	
	D_{1cc} (Gy)	$D_{30\%}$ (Gy)	D_{1cc} (Gy)	D_{2cc} (Gy)	D_{1cc} (Gy)	D_{2cc} (Gy)
MA	19.34	17.40	15.89	19.17	10.01	10.95
GS	19.06	16.63	11.82	13.89	10.60	11.80

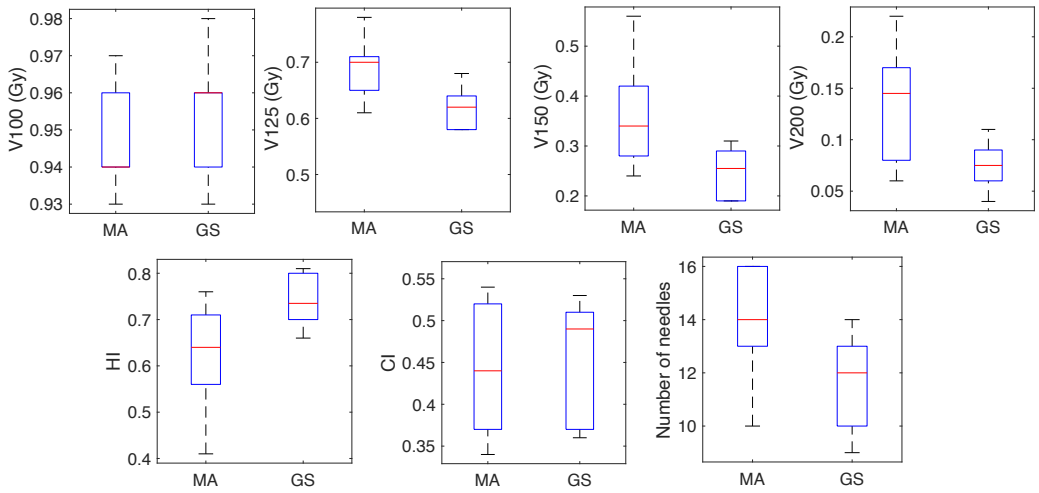

Figure 5: Boxplot of PTV coverage metrics and number of needle catheters.

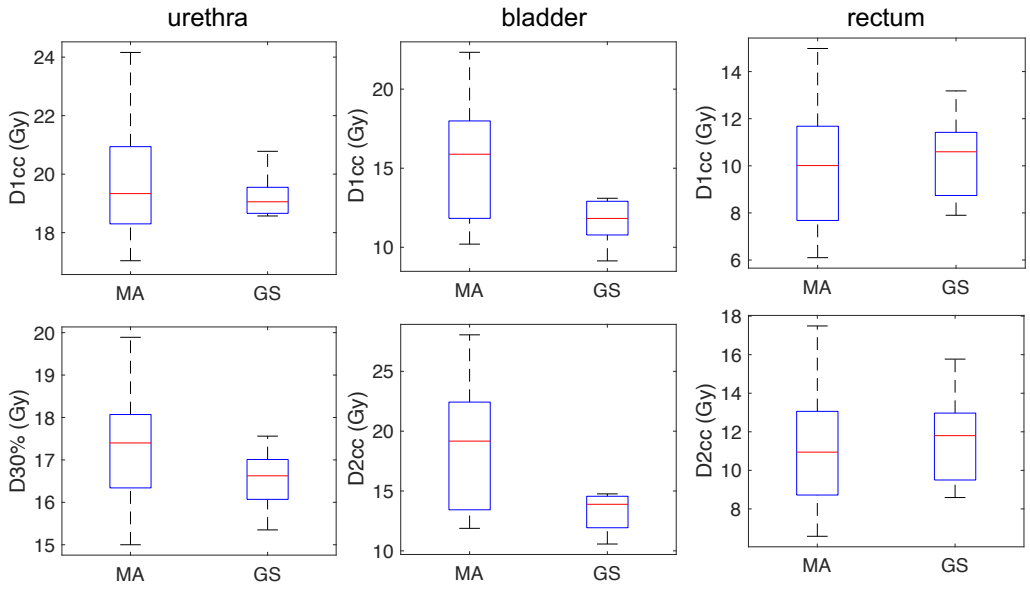

Figure 6: Boxplot on dosimetric quantities of interest for OARs: urethra (left column), bladder (middle column), and rectum (right column).

4. CONCLUSION AND DISCUSSIONS

In this work, we propose a method for simultaneous needle catheter selection and dwell time optimization for the preplanning task of prostate cancer HDR brachytherapy. The method was based on group sparsity. It introduced a weighed $L_{2,1}$ penalty term in the objective function to promote sparsity with respect to the number of active needle catheters. We further propose an adaptive weight adjustment approach to heuristically adjust needle weights during the iterative optimization process to enable more effective selection of needle catheters. The proposed method was tested on ten patient cases. Compared with plans optimized based on pre-determined needle catheter positions manually selected by physicians, the proposed method was able to effectively select needle catheters yielding plans with better PTV coverage and OAR sparing in most of dosimetric variables of interest. More importantly, the improvement of plan quality was achieved with two less needle catheters as compared to the plans with manually selected needle catheter positions.

In our optimization scheme, there were several parameters, including the step size for the proximal operator β, the overall relative weight c between the dosimetric objectives and the sparsity objective, and $\lambda_i, i = 1, \dots, M$, the relative important among organs. Generally speaking, the selections of these parameters affect the resulting plan quality and number of needle catheters. Hence, it is worthwhile to discuss this parameter selection issue. The parameter β can be determined by the Lipchitz gradient constant of the function f according to (Boyd *et al.*, 2004). Once its value was set small enough, it does not affect the solution but only the convergence speed. In our study, we set the parameter $\beta = 1/L$, where L is the Lipchitz gradient constant of f, which can be numerically computed given its function form. The parameter c governs the tradeoff between the planning dosimetry objectives and the needle catheter number objective. The parameters $\lambda_i, i = 1, \dots, M$

control different objectives among the PTV and OARs. The proper values of these parameters are case dependent. In this work, these parameter values are adjusted manually to yield a satisfactory solution for each patient case. This manual selection limits the proposed method, as it would affect the practicality of the method for routine clinical use. Future studies to solve this problem are needed and are being explored by our group. A possible solution is to solve the optimization problem in real time, which would allow a user to visualize the resulting plan quality as a function of the parameter values and interactively adjust them to achieve optimal results. Alternatively, it may be possible to build a statistical model to relate the patient anatomy to the optimal parameter values. This approach has been previously explored in the context of plan optimization for intensity modulated radiation therapy (Lee *et al.*, 2013; Boutilier *et al.*, 2015) and we expect extension of this method to our problem is feasible. In addition, recent advances in deep reinforcement learning (Shen *et al.*, 2020b) may help in solving this problem. Studies have demonstrated feasibility of using deep reinforcement learning to model human intuition in adjusting parameters of objective functions for optimization problems, such as in iterative CT reconstruction (Shen *et al.*, 2018; Shen *et al.*, 2019b) and radiotherapy treatment planning (Shen *et al.*, 2019a; Shen *et al.*, 2020a).

As a method for preplanning, the proposed algorithm assumes ideal needle catheter placement in the patient body, i.e. without considering practical issues such as the bending of needle catheters or other uncertainties in needle catheter placement during the insertion process. Hence, its clinical value may be limited to a certain extent. The calculated needle catheter positions assuming the ideal insertion situation may not be optimal anymore once the needle catheters deviate from these conditions. An approach to potentially alleviate this caveat is to further extend the proposed needle catheter selection method to a real-time guidance form. Specifically, the method would be executed continuously during a needle insertion procedure. At any given time, the needle catheters already inserted are known to the algorithm, and the algorithm would optimize with respect to remaining needle catheter positions to select the needle catheter positions based on those already inserted needle catheters. This is a feasible approach, as the procedure is often performed under real-time image guidance, and digitization of inserted needle catheter position during the procedure is achievable.

There are also other potential areas of applications of the proposed algorithm. such as HDR brachytherapy for cervical cancer when using interstitial needle catheters (Nag *et al.*, 2000). The planning problems in these cases face the same challenge of achieving sufficient dosimetric coverage while minimizing the use of needle catheters to reduce trauma. It is expected that it is straightforward to extend the current algorithm in those contexts. Similarly, the algorithm may also be extended to preplanning for LDR brachytherapy of prostate cancer and other tumor sites.

Reference

Ahmad R and Schniter P 2015 Iteratively Reweighted l_1 Approaches to Sparse Composite Regularization *IEEE transactions on computational imaging* **1** 220-35

Bach F, Jenatton R, Mairal J and Obozinski G 2012 Optimization with sparsity-inducing penalties *Foundations and Trends® in Machine Learning* **4** 1-106

Bach F R 2008 Consistency of the group lasso and multiple kernel learning *Journal of Machine Learning Research* **9** 1179-225

Beck A and Teboulle M 2009 A fast iterative shrinkage-thresholding algorithm for linear inverse problems *Siam J Imaging Sci* **2** 183-202

Blasko J C, Mate T, Sylvester J E, Grimm P D and Cavanagh W 2002 Brachytherapy for carcinoma of the prostate: techniques, patient selection, and clinical outcomes *Semin Radiat Oncol* **12** 81-94

Boutilier J J, Lee T, Craig T, Sharpe M B and Chan T C 2015 Models for predicting objective function weights in prostate cancer IMRT *Medical physics* **42** 1586-95

Boyd S, Boyd S P and Vandenberghe L 2004 *Convex optimization*: Cambridge university press)

Boyea G, Antonucci J, Wallace M, Ghilezan M, Gustafson G, Chen P Y, Saputo K, Flynn C and Martinez A 2007 The role of needle trauma in the development of urinary toxicity following prostate High Dose Rate (HDR) Brachytherapy *Int J Radiat Oncol* **69** S357-S8

Breedveld S, Bennan A B, Aluwini S, Schaart D R, Kolkman-Deurloo I-K K and Heijmen B J 2019 Fast automated multi-criteria planning for HDR brachytherapy explored for prostate cancer *Physics in Medicine & Biology* **64** 205002

Cirino E, Iftimia I and Lo T 2012 Using Dose Homogeneity Index and Conformity Index to Evaluate Prostate High-dose-rate Plan Quality and Consistency *International Journal of Radiation Oncology• Biology• Physics* **84** S770-S1

Deist T M and Gorissen B L 2016 High-dose-rate prostate brachytherapy inverse planning on dose-volume criteria by simulated annealing *Phys Med Biol* **61** 1155-70

Dinges S, Deger S, Koswig S, Boehmer D, Schnorr D, Wiegel T, Loening S A, Dietel M, Hinkelbein W and Budach V 1998 High-dose rate interstitial with external beam irradiation for localized prostate cancer--results of a prospective trial *Radiother Oncol* **48** 197-202

Eapen L, Kayser C, Deshaies Y, Perry G, Choan E, Morash C, Cygler J E, Wilkins D and Dahrouge S 2004 Correlating the degree of needle trauma during prostate brachytherapy and the development of acute urinary toxicity *Int J Radiat Oncol* **59** 1392-4

Galalae R M, Kovacs G, Schultze J, Loch T, Rzehak P, Wilhelm R, Bertermann H, Buschbeck B, Kohr P and Kimmig B 2002 Long-term outcome after elective irradiation of the pelvic lymphatics and local dose escalation using high-dose-rate brachytherapy for locally advanced prostate cancer *Int J Radiat Oncol Biol Phys* **52** 81-90

Gu W, Neph R, Ruan D, Zou W, Dong L and Sheng K 2019 Robust beam orientation optimization for intensity‐modulated proton therapy *Medical physics* **46** 3356-70

Gu W, O'Connor D, Nguyen D, Yu V Y, Ruan D, Dong L and Sheng K 2018 Integrated beam orientation and scanning‐spot optimization in intensity‐modulated proton therapy for brain and unilateral head and neck tumors *Medical physics* **45** 1338-50

Huang J and Zhang T 2010 The benefit of group sparsity *The Annals of Statistics* **38** 1978-2004

Jia X, Men C, Lou Y and Jiang S B 2011 Beam orientation optimization for intensity modulated radiation therapy using adaptive l2, 1-minimization *Physics in Medicine & Biology* **56** 6205

Lachance B, Beliveau-Nadeau D, Lessard E, Chretien M, Hsu I C, Pouliot J, Beaulieu L and Vigneault E 2002 Early clinical experience with anatomy-based inverse planning dose optimization for high-dose-rate boost of the prostate *Int J Radiat Oncol Biol Phys* **54** 86-100

Lee T, Hammad M, Chan T C, Craig T and Sharpe M B 2013 Predicting objective function weights from patient anatomy in prostate IMRT treatment planning *Medical physics* **40** 121706

Lessard E and Pouliot J 2001 Inverse planning anatomy-based dose optimization for HDR-brachytherapy of the prostate using fast simulated annealing algorithm and dedicated objective function *Med Phys* **28** 773-9

Li Y, Zhang J, Fan S, Yang J, Xiong J, Cheng X, Sari H, Adachi F and Gui G 2017 Sparse adaptive iteratively-weighted thresholding algorithm (SAITA) for L p-regularization using the multiple sub-dictionary representation *Sensors* **17** 2920

Luong N H, Alderliesten T, Pieters B R, Bel A, Niatsetski Y and Bosman P A 2019 Fast and insightful bi-objective optimization for prostate cancer treatment planning with high-dose-rate brachytherapy *Applied Soft Computing* **84** 105681

Major T, Polgár C, Jorgo K, Stelczer G and Agoston P 2017 Dosimetric comparison between treatment plans of patients treated with low-dose-rate vs. high-dose-rate interstitial prostate brachytherapy as monotherapy: Initial findings of a randomized clinical trial *Brachytherapy* **16** 608-15

Martinez A A, Pataki I, Edmundson G, Sebastian E, Brabbins D and Gustafson G 2001 Phase II prospective study of the use of conformal high-dose-rate brachytherapy as monotherapy for the treatment of favorable stage prostate cancer: A feasibility report *Int J Radiat Oncol* **49** 61-9

Mate T P, Gottesman J E, Hatton J, Gribble M and Van Hollebeke L 1998 High dose-rate afterloading (192)Iridium prostate brachytherapy: Feasibility report *Int J Radiat Oncol* **41** 525-33

Meier L, Van De Geer S and Bühlmann P 2008 The group lasso for logistic regression *Journal of the Royal Statistical Society: Series B (Statistical Methodology)* **70** 53-71

Moren B, Larsson T and Carlsson Tedgren A 2018 Mathematical optimization of high dose-rate brachytherapy-derivation of a linear penalty model from a dose-volume model *Phys Med Biol* **63** 065011

Moren B, Larsson T and Carlsson Tedgren A 2019 An extended dose-volume model in high dose-rate brachytherapy - Using mean-tail-dose to reduce tumor underdosage *Med Phys* **46** 2556-66

Nag S, Erickson B, Thomadsen B, Orton C, Demanes J D, Petereit D and Society A B 2000 The American Brachytherapy Society recommendations for high-dose-rate brachytherapy for carcinoma of the cervix *International Journal of Radiation Oncology* Biology* Physics* **48** 201-11

O'Connor D, Voronenko Y, Nguyen D, Yin W and Sheng K 2017 Fast non-coplanar beam orientation optimization based on group sparsity *arXiv preprint arXiv:1710.05308*

Parvaresh F, Vikalo H, Misra S and Hassibi B 2008 Recovering sparse signals using sparse measurement matrices in compressed DNA microarrays *IEEE Journal of Selected Topics in Signal Processing* **2** 275-85

Rivard M J, Coursey B M, DeWerd L A, Hanson W F, Huq M S, Ibbott G S, Mitch M G, Nath R and Williamson J F 2004 Update of AAPM Task Group No. 43 Report: A revised AAPM protocol for brachytherapy dose calculations *Medical Physics* **31** 633-74

Sadowski K L, van der Meer M C, Luong N H, Alderliesten T, Thierens D, van der Laarse R, Niatsetski Y, Bel A and Bosman P A 2017 *Exploring trade-offs between target coverage, healthy tissue sparing, and the placement of catheters in HDR brachytherapy for prostate cancer using a novel multi-objective model-based mixed-integer evolutionary algorithm*. Published *Proceedings of the Genetic and Evolutionary Computation Conference,2017),* vol. Series*)* pp 1224-31

Shen C, Gonzalez Y, Chen L, Jiang S B and Jia X 2018 Intelligent parameter tuning in optimization-based iterative CT reconstruction via deep reinforcement learning *IEEE transactions on medical imaging* **37** 1430-9

Shen C, Gonzalez Y, Klages P, Qin N, Jung H, Chen L, Nguyen D, Jiang S B and Jia X 2019a Intelligent inverse treatment planning via deep reinforcement learning, a proof-of-principle study in high dose-rate brachytherapy for cervical cancer *Physics in Medicine & Biology* **64** 115013

Shen C, Nguyen D, Chen L, Gonzalez Y, McBeth R, Qin N, Jiang S B and Jia X 2020a Operating a treatment planning system using a deep‐reinforcement learning‐based virtual

treatment planner for prostate cancer intensity‐modulated radiation therapy treatment planning *Medical physics*

Shen C, Nguyen D, Zhou Z, Jiang S B, Dong B and Jia X 2020b An introduction to deep learning in medical physics: advantages, potential, and challenges *Physics in Medicine & Biology* **65** 05TR1

Shen C, Tsai M-Y, Gonzalez Y, Chen L, Jiang S B and Jia X 2019b *Quality-guided deep reinforcement learning for parameter tuning in iterative CT reconstruction*. Published *15th International Meeting on Fully Three-Dimensional Image Reconstruction in Radiology and Nuclear Medicine,2019b),* vol. Series 11072*)*: International Society for Optics and Photonics) p 1107203

Siauw T, Cunha A, Atamtürk A, Hsu I C, Pouliot J and Goldberg K 2011 IPIP: A new approach to inverse planning for HDR brachytherapy by directly optimizing dosimetric indices *Medical Physics* **38** 4045-51

Siauw T, Cunha A, Berenson D, Atamtürk A, Hsu I C, Goldberg K and Pouliot J 2012 NPIP: A skew line needle configuration optimization system for HDR brachytherapy *Medical physics* **39** 4339-46

Simon N, Friedman J, Hastie T and Tibshirani R 2013 A sparse-group lasso *Journal of computational and graphical statistics* **22** 231-45

Thompson I, Thrasher J B, Aus G, Burnett A L, Canby-Hagino E D, Cookson M S, D'Amico A V, Dmochowski R R, Eton D T, Forman J D, Goldenberg S L, Hernandez J, Higano C S, Kraus S R, Moul J W and Tangen C M 2007 Guideline for the management of clinically localized prostate cancer: 2007 update *J Urology* **177** 2106-31

van der Meer M C, Pieters B R, Niatsetski Y, Alderliesten T, Bel A and Bosman P A 2018 *Better and faster catheter position optimization in HDR brachytherapy for prostate cancer using multi-objective real-valued GOMEA*. Published *Proceedings of the Genetic and Evolutionary Computation Conference,2018),* vol. Series*)* pp 1387-94

Wu C-J and Lin D W 2006 *A group matching pursuit algorithm for sparse channel estimation for OFDM transmission*. Published *2006 IEEE International Conference on Acoustics Speech and Signal Processing Proceedings,2006),* vol. Series 4*)*: IEEE) pp IV-IV

Yoshioka Y, Nose T, Yoshida K, Inoue T, Yamazaki H, Tanaka E, Shiomi H, Imai A, Nakamura S, Shimamoto S and Inoue T 2000 High-dose-rate interstitial brachytherapy as a monotherapy for localized prostate cancer: treatment description and preliminary results of a phase I/II clinical trial *Int J Radiat Oncol Biol Phys* **48** 675-81